Benzamil inhibits neuronal and heterologously expressed small conductance Ca^{2+}-activated K^+ channels

Marisol Sampedro Castañeda[1,3], Raffaella Tonini[1,2] , Christopher D. Richards[1], Martin Stocker[1*] and Paola Pedarzani[1*]

[1]Research Department of Neuroscience, Physiology and Pharmacology, University College London, London, UK.

[2]Neuromodulation of Cortical and Subcortical Circuits Laboratory, Fondazione Istituto Italiano di Tecnologia, Genova, Italy.

[3]Kinases and Brain Development Laboratory, The Francis Crick Institute, London, UK

ORCID:

Paola Pedarzani - https://orcid.org/0000-0002-2665-7911

Martin Stocker - https://orcid.org/0000-0003-3993-5666

*To whom correspondence should be addressed at:

Research Department of Neuroscience, Physiology and Pharmacology

University College London, Gower Street, London WC1E 6BT, United Kingdom

Tel.: +44-(0)20-7679-7744 (PP) or +44-(0)20-3549-5671(MS)

E-mail: p.pedarzani@ucl.ac.uk or m.stocker@ucl.ac.uk

Abstract

Small conductance Ca^{2+}-activated K^+ (SK) channels are expressed throughout the soma and dendrites of pyramidal neurons in the neocortex and hippocampal formation, where they participate in the local regulation of membrane excitability and synaptic signals. Through their inter-play with Ca^{2+} channels, SK channels regulate Ca^{2+} influx triggered by back-propagating action potentials in dendrites. Inhibition of SK channels affects both the amplitude and duration of Ca^{2+} transients, but the role of Ca^{2+} clearance mechanisms and their link to SK channel activity has not been established. Here we report the effect of the Na^+/Ca^{2+} exchanger (NCX) inhibitor benzamil on Ca^{2+} extrusion and SK channels in the regulation of dendritic Ca^{2+} signals. Benzamil increased the duration and amplitude of dendritic Ca^{2+} transients elicited by back-propagating action potentials in hippocampal pyramidal neurons. This data is consistent with previous studies with SK channel blockers and suggests that benzamil inhibits SK channels in addition to the Na^+/Ca^{2+} exchanger. Here we show that indeed both the neuronal SK-mediated I_{AHP} current and the currents mediated by heterologously expressed SK channels were inhibited by benzamil. The inhibition of recombinant SK channels was seen with different K^+ concentration gradients, and was stronger at negative voltages. The suppression of SK channels by benzamil is consistent with previous findings on the modulation of Ca^{2+} signals by SK channels in neurons. We additionally show that benzamil inhibits neuronal voltage-gated calcium currents. The results prompt a careful reassessment of the effects of benzamil on Ca^{2+} transients in native systems, given the spectrum of ion channels and exchangers this compound targets within a similar range of concentrations.

Keywords: benzamil; SK channel; hippocampal neuron; backpropagating action potential; calcium transient; calcium extrusion.

Introduction

Calcium signalling and homeostasis are critical determinants of neuronal excitability, neuronal energy metabolism, neurotransmission and synaptic function. Transient elevations of cytosolic Ca^{2+} are generated in response to the activation of plasma membrane-standing receptors and ion channels or the release of Ca^{2+} from intracellular stores, such as the endoplasmic reticulum (ER). The amplitude, duration and spatial distribution of neuronal, cytosolic Ca^{2+} transients are tightly controlled and regulated by cytoplasmic Ca^{2+} binding proteins, Ca^{2+} uptake by mitochondria and the ER, as well as Ca^{2+} extrusion by PMCA (plasma membrane Ca^{2+} ATP-ases) and Na^{+}/Ca^{2+} exchangers in the plasma membrane (Brini et al., 2014).

The spatial and temporal dynamics of neuronal Ca^{2+} signals are further shaped by feedback mechanisms, which limit additional entry of Ca^{2+} after an initial increase. A further raise in Ca^{2+} can be impeded if the entry process is coupled in space and time with a hyperpolarizing event counteracting it. One class of molecules regulating intracellular Ca^{2+} transients are small conductance Ca^{2+}-activated potassium channels (SK). These channels have been shown to limit Ca^{2+} entry through ligand- and voltage-gated Ca^{2+}-permeable channels in different neuronal compartments. Thus, the activation of SK channels limits the influx of Ca^{2+} through NMDA receptors and decreases glutamatergic excitatory postsynaptic potentials in dendritic spines of hippocampal (Bloodgood and Sabatini, 2007; Jones et al., 2017; Ngo-Anh et al., 2005), neocortical (Faber, 2010; Jones et al., 2017), amygdala (Faber, 2010) and striatal neurons (Higley and Sabatini, 2010). Their activation also controls the duration of glutamate-induced Ca^{2+} plateau potentials in distal apical dendrites of hippocampal neurons (Cai et al., 2004), and regulates the amplitude of Ca^{2+} transients elicited by back-propagating action potentials in the proximal portion of apical dendrites of hippocampal neurons (Tonini et al., 2013), in dendrites of striatal medium spiny neurons (Trusel et al., 2015), and in spines and dendritic shafts of neocortical pyramidal neurons (Jones and Stuart, 2013; Rudolph and Thanawala, 2015). It has further been suggested that in thalamic neurons SK channels modulate the duration of Ca^{2+} transients by competing for available Ca^{2+} with the sarco/endoplasmic reticulum Ca^{2+} ATP-ase (SERCA) (Cueni et al., 2008). SK channels might also indirectly regulate the activity of PMCA and Na^{+}/Ca^{2+} exchangers through their modulation of Ca^{2+} transients (Scheuss et al., 2006). The orchestrated action of Ca^{2+} sources, functionally coupled Ca^{2+}-activated ion channels and Ca^{2+} extrusion mechanisms is therefore emerging as a fundamental interplay shaping Ca^{2+} signals in neurons.

The availability of specific and selective pharmacological tools is crucial to dissect the contribution of different extrusion mechanisms to this interplay and regulation of neuronal Ca^{2+} signals. The amiloride analogue benzamil (3,5-diamino-N-[(1E)- amino(benzylamino)methyl

idene]-6-chloropyrazine-2-carboxamide) was one of the first relatively potent inhibitors of Na^+/Ca^{2+} exchange to be described (Jurkowitz et al., 1983; Kaczorowski et al., 1985; for a review see Kaczorowski et al., 1988; Siegl et al., 1984), and has been extensively used to investigate the role of Na^+/Ca^{2+} exchanger of the NCX family in mediating Ca^{2+} extrusion in several types of neurons under normal and pathological conditions. Thus, one of the first pharmacological characterisations of Na^+/Ca^{2+} exchange in a neuronal preparation showed that 270 μM benzamil inhibited Na^+/Ca^{2+} exchange in rat brain synaptosomes by half (Schellenberg et al., 1985). This opened the way for the use of benzamil to investigate the role of Na^+/Ca^{2+} exchanger in Ca^{2+} clearance following back-propagation of action potentials in proximal dendrites in layer V neocortical pyramidal neurons (Markram et al., 1995), synapse-specific Ca^{2+} influx through Ca^{2+}-permeable AMPA receptors in the dendrites of aspiny cortical interneurones (Goldberg et al., 2003), and Ca^{2+} transients elicited by synaptic stimulation in spines and dendritic shafts of CA1 pyramidal neurons (Lorincz et al., 2007). Several studies have further addressed the role of Na^+/Ca^{2+} exchangers in response to ischemia and anoxia in hippocampal neurons (Fung and Haddad, 1997; Lobner and Lipton, 1993; Uchikado et al., 2000) and epileptic activity in subicular neurons (Srinivas and Sikdar, 2008). In all these studies benzamil was used in a concentration range of 30-500 μM.

However, in this concentration range benzamil targets several other ion channels, exchangers and receptors, including for example L- and T-type voltage-gated Ca^{2+} channels (Garcia et al., 1990), epithelial Na^+ channels (Cuthbert, 1976; Kleyman and Cragoe, 1988; McNicholas and Canessa, 1997), TTX-sensitive Na^+ channels (Kleyman and Cragoe, 1988), H^+-gated acid-sensing ion channels (ASIC, Page et al., 2007), mechanosensitive channels (Lane et al., 1992; Rusch et al., 1994), TRPP3 channels (Dai et al., 2007), Na^+/H^+ exchangers (Kapus et al., 1988; Yu et al., 1993), and nicotinic acetylcholine receptors (reviewed by Kleyman and Cragoe, 1988; Santos-Torres et al., 2011). The action of benzamil on various molecular targets, many of which are expressed in neurons and are part of the Ca^{2+} signalling toolkit, needs therefore to be carefully considered when drawing conclusions on its action on Ca^{2+} extrusion through the inhibition of Na^+/Ca^{2+} exchange.

With this in mind, to elucidate the interplay between dendritic Ca^{2+} sources, SK channels and Ca^{2+} extrusion mechanisms in hippocampal neurons, we investigated the specificity of action of benzamil, and in particular its potential effect on SK channels. We show that benzamil directly inhibits recombinant and neuronal SK mediated currents. Our results suggest that caution must be exercised in assessing the impact of Ca^{2+} extrusion mediated by Na^+/Ca^{2+} exchange on neuronal Ca^{2+} transients by using benzamil, as part of the effects of this compound could be mediated by SK channel inhibition.

Methods

Primary neuronal culture

Primary hippocampal cultures were prepared from P0 male and female Sprague Dawley rats as previously described (Tonini et al., 2013) and in accordance with the UK Animals (Scientific Procedures) Act 1986; protocols were reviewed and approved by the UCL Animal Welfare and Ethical Review Body. Briefly, after dissection of the hippocampus, 2.5% trypsin (Invitrogen, Paisley, UK) was applied and the tissue mechanically dissociated using polished glass Pasteur pipettes. Cells were plated onto poly-D-lysine (100 μg/ml, Sigma-Aldrich, Dorset, UK)-coated glass coverslips at a density of 18,500 – 23,500 viable cells/cm^2 and allowed to settle in Minimal Essential Medium supplemented with 10 % Horse Serum, 1 mM pyruvic acid, 2 mM glutamine (all from Gibco, Paisley, UK), and 0.6% glucose (Sigma-Aldrich, Dorset, UK) in a humidified incubator at 37˚C in 5% CO_2. This attachment solution was replaced after 4-14h with Neurobasal medium (Gibco, Paisley, UK) containing 2 % B27 supplement (Gibco, Paisley, UK), 2 mM glutamine (Gibco, Paisley, UK), 0.6 % glucose and penicillin/streptomycin (100 U/ml/100 μg/ml, Sigma-Aldrich, Dorset, UK). Cultures were grown for 10-12 days before conducting imaging or electrophysiological experiments and the growth medium was replaced every 5-7 days.

Electrophysiological recordings from hippocampal neurons.

Whole-cell patch clamp recordings from morphologically identified hippocampal neurons in primary hippocampal cultures were performed using an EPC10 (HEKA, Lambrecht, Germany) or Axopatch 1-D amplifier (Axon Instruments, Foster City, California). Data were acquired with Pulse v8.8 software (HEKA, Lambrecht, Germany) or with the Strathclyde Electrophysiology Software v.3.2.9 (J. Dempster, University of Strathclyde, UK). Recordings were made at room temperature (20-22˚C).

For voltage-clamp experiments cells were perfused at a flow rate of 2 ml/min with extracellular solution containing (in mM): 140 NaCl, 3.5 KCl, 10 HEPES, 16 Glucose, 2 $CaCl_2$ and 1.5 $MgCl_2$ (pH 7.4 with NaOH, 305-310 mOsm/kg). Pipettes were pulled from borosilicate glass (Kimax, Kimble Chase, Mexico) and had a resistance of 3-5 MΩ when filled with intracellular solution (in mM): 135 $KMeSO_4$, 10 KCl, 10 HEPES, 1 $MgCl_2$, 2 Na_2-ATP, 0.4 Na_3-GTP (pH 7.2-7.3 with KOH, 280-290 mOsm/kg). 8-CPT-cAMP (50 μM) was included in the pipette solution in order to measure the apamin sensitive I_{AHP} current, also referred to as mI_{AHP} or I_{mAHP}, in isolation. I_{AHP} was measured as an outward current at -50 mV, following a 200 ms-long depolarizing voltage step to +30 mV to activate voltage-gated Ca^{2+} channels, in the

presence of tetrodotoxin (TTX, 0.5 μM), tetraethylammonium (TEA, 1 mM), DL-AP5 (5 μM) and NBQX (25 μM) at a frequency of 0.033 Hz. Series resistance (range 15-25 MΩ) was monitored at regular intervals throughout the recordings and only cells that presented minimal variations (≤15%) were included. Data were filtered at 1 kHz and digitized at 4 kHz and reported without corrections for a liquid junction potential (9 mV).

For current clamp recordings coverslips were continuously superfused with external solution (2.5 ml/min) containing (in mM): 140 NaCl, 3.5 KCl, 10 HEPES, 20 Glucose, 1.5 $CaCl_2$ and 1.5 $MgCl_2$ (pH 7.4 with NaOH, 300-305 mOsm/kg). Patch electrodes (5-6 MΩ, TW100F-4 glass, World Precision Instruments, USA) were filled with the same intracellular solution as for voltage clamp recordings (see above). Trains of four action potentials were elicited in response to four 10 ms-long pulses at 20 Hz in the presence DL-AP5 (25 μM) and NBQX (5 μM). The membrane potential was maintained at -60 mV between stimulations. The resting membrane potential was frequently checked and only neurons with a stable resting potential more hyperpolarized than -50 mV were included in the analysis. Data were filtered at 10 kHz and digitized at 20 kHz.

For voltage-clamp measurements of voltage-gated calcium currents, transverse hippocampal slices (400 μm thick) were prepared from young (postnatal day 6-7 (P6-P7)) male and female Sprague-Dawley rats. Whole-cell gigaseal recordings were obtained from CA1 pyramidal cells in the slice by using the ‘‘blind’’ method (Blanton et al., 1989) using an EPC10 (HEKA, Lambrecht, Germany). Data were acquired with Pulse v8.8 software (HEKA, Lambrecht, Germany). Recordings were made at room temperature (20-22˚C).

For measurements of calcium currents, slices were perfused at a flow rate of 2 ml/min with extracellular solution containing (in mM): 110 NaCl, 10 tetraethylammonium chloride (TEA), 1.25 KCl, 1.25 KH_2PO_4, 25 $NaHCO_3$, 16 Glucose, 1.5 $CaCl_2$ and 1.5 $MgCl_2$ (pH 7.4 with NaOH, 305-310 mOsm/kg). Pipettes were pulled from borosilicate glass (Hilgenberg, Germany) and had a resistance of 4.6-5.6 MΩ when filled with intracellular solution (in mM): 100 Cs-gluconate, 10 CsCl, 10 HEPES, 1 $MgCl_2$, 2 Na_2-ATP, 10 EGTA, 20 Na_2-creatine (pH 7.25 with CsOH, 280 mOsm/kg). The voltage-gated calcium current was measured as an inward current at +5 mV in response to a 150 ms-long depolarizing voltage step from a holding potential of -50 mV, in the presence of tetrodotoxin (TTX, 0.5 μM), 4-aminopyridine (4-AP, 5 mM) and CsCl (5 mM) at a frequency of 0.05 Hz. Data were filtered at 1.56 kHz and digitised at 6.25 kHz.

Maintenance of HEK293 cells stably expressing SK channels

The HEK293 cell lines stably expressing small conductance Ca^{2+} activated potassium channels used in this study were generated as previously described; hSK1 ($hK_{Ca}2.1$) (Nolting et al., 2007) and rSK2 ($rK_{Ca}2.2$) and rSK3 ($rK_{Ca}2.3$) (Pedarzani et al., 2002). Cell lines were kept in a humidified atmosphere (5% CO_2, 95% air) at 37 °C in Dulbecco's modified Eagle's medium/F12 (Gibco, Paisley, UK) supplemented with 2 mM L-glutamine, 10% fetal calf serum (Gibco, Paisley, UK), penicillin/streptomycin 100 U/ml/100 µg/ml and the appropriate selection antibiotic (hSK1: hygromycin B; rSK2, rSK3: G418). Upon reaching 95% confluence, cells were trypsinized, plated on glass coverslips and used for electrophysiological recordings 20-48 hours after.

Electrophysiological recordings of HEK293 cells

Whole-cell patch clamp recordings of HEK293 cells expressing SK channels were performed using an EPC10 (HEKA, Lambrecht, Germany) amplifier. Data were acquired with Pulse (v8.8) software (HEKA, Lambrecht, Germany). Pipettes were pulled from borosilicate glass (Kimax, Kimble Chase, Mexico) and had a resistance of 1.2-2.7 MOhm when filled with intracellular solution (see below).

SK channels were activated by whole-cell dialysis with an intracellular solution containing (in mM): 130 $KMeSO_4$, 10 HEPES, 10 EGTA, (pH7.2 with KOH, 285-290 mOsmol/kg H_2O). Sufficient $MgCl_2$ and $CaCl_2$ were added to obtain free metal concentrations of Mg^{2+} (1 mM) and Ca^{2+} (1 µM) based on calculations using the program MaxChelator (Webmaxc Extended, Stanford, USA). Cells were perfused with 1.5 ml/min of either a high K^+ extracellular solution containing (in mM): 144 KCl, 10 HEPES, 2 $CaCl_2$, 1 $MgCl_2$, 10 D-glucose (pH 7.4 with KOH, 305-310 mOsmol/kg H_2O) or a physiological extracellular K^+ solution containing (in mM): 4 KCl, 140 NaCl, 2 $CaCl_2$, 1 $MgCl_2$, 10 HEPES, 10 Glucose (pH 7.4 with NaOH, 305-310 mOsmol/kg H_2O).

Currents were recorded by ramping (400 ms) the voltage from -140 to +60 mV at room temperature (22˚C). Data were filtered at 5 kHz and digitized at 20 kHz. Voltage-clamp errors due to large current sizes as well as a liquid junction potential of 4.5 mV were corrected off-line. Currents not due to SK channel activation were revealed upon inhibition of the SK mediated current by d-tubocurarine (0.2-1 mM) at the end of every recording and only cells with a residual current of less than 10% of the maximal current amplitude at -80 mV were included. To allow for realistic comparison between experimental conditions the residual current was subtracted.

Two-photon Ca^{2+} imaging experiments

Two photon Ca^{2+} imaging was performed with a Bio-Rad multiphoton microscope based on a 1024 scan head installed on a Nikon E600FN upright microscope with a mounted recording chamber and a Nikon 60x NA 1.0 water-immersion objective. A Millennia V pump laser coupled to a mode-locked Ti:sapphire infra-red laser (Tsunami, Spectra Physics) was used for fluorescence excitation, tuned to 790 nm. Imaging parameters and controls were as described previously (Tonini et al., 2013). In short to observe Ca^{2+} transients, 20 μM Fluo-4 (Molecular Probes, Eugene, Oregon) was dissolved in the intracellular recording solution. Upon achieving the whole-cell configuration, the dye was allowed to equilibrate for 10-15 min in the proximal dendrites of the imaged neuron. Line scans images (Lasersharp software; Bio-Rad, UK) triggered by electrical stimuli delivered at the soma were collected from proximal apical processes (<50 μm from the soma) at 6 ms intervals.

Data Analysis and Statistics

Imaging analysis was performed as described previously (Tonini et al., 2013) using ImageJ (NIH) and Origin 7.0 (Microcal software). After subtraction of background fluorescence, the basal fluorescence (F_{basal}) was measured. In control conditions F_{basal} did not change by more than twice the standard deviation throughout the experiment. The amplitude of the fluorescence transient at the recording site was expressed as the fractional change in basal fluorescence $(F-F_{basal})/F_{basal}=(\Delta F/F)$, which is approximately proportional to the changes in intracellular Ca^{2+}. For data analysis, transients were digitally filtered off-line (adjacent-averaging routine, smoothing factor n = 5, Origin 7) and peak fluorescence was calculated averaging data points 30-60 ms around the maximum. The decay time course of Ca^{2+} transients was fitted by a single-exponential function.

Current clamp data were analyzed by pClamp9 Clampfit routine (Axon Instruments, California, USA) and Origin. Voltage clamp data was processed in Pulsefit v8.5 (HEKA, Germany), Igor v6.12 (Wavemetrics, Oregon, USA) and Prism v4 (GraphPad Software Inc., San Diego, USA). The I_{AHP} amplitude was measured around 100 ms following the depolarizing step. The decay time course was fitted by a single exponential function. The amplitude of calcium currents was measured at the peak, before and after 7.8 ± 0.8 minute-long benzamil (30 μM) application.

The data points shown for the concentration-response curve represent mean response values. However, the data points for the fit were obtained from individual HEK293 cells and are as such individual replicates. Consequently the concentration-response curve was obtained by fitting to: $I/I_{max}=(1-a_0)/(1+([inhibitor]/IC_{50})^h)+a_0$, where h is the Hill coefficient and IC_{50} the concentration of inhibitor that produces half maximal inhibition. The curve minimum (a_0) was not fixed. SK

channel rectification was quantified as the ratio between whole-cell currents at -40 and +40 mV, where the current voltage response was respectively linear and maximally rectifying under our experimental conditions.

Two tailed Student's t-tests (paired or unpaired) and one or two way Analysis of Variance were used for statistical comparisons (Prism v4; α=0.05) and values are reported as mean ± SEM or confidence interval (95 % CI).

Chemicals

Amiloride hydrochloride was obtained from Abcam (Cambridge, UK); ATP di-sodium from Sigma-Aldrich (Dorset, UK); benzamil hydrochloride and 8-(4-chlorophenylthio)adenosine 3',5'-cyclic monophosphate (CPT-cAMP) from Sigma-Aldrich (Dorset, UK); DL-2-Amino-5-phosphonopentanoic acid sodium salt (DL-AP5), d-Tubocurarine and 2,3-Dioxo-6-nitro-1,2,3,4-tetrahydrobenzo[*f*]quinoxaline-7-sulfonamide disodium salt (NBQX) from Tocris Bioscience (Bristol, UK) or Ascent Scientific (Weston-super-Mare, UK); Fluo-4 Pentapotassium Salt from Molecular Probes (Eugene, OR); GTP tri-sodium, Na_2-creatine, 4-aminopyridine and tetraethylammonium (TEA) from Sigma-Aldrich (Dorset, UK); $KMeSO_4$ from Fisher Scientific (Loughborough, UK); tetrodotoxin (TTX) citrate-free from Latoxan (Rosans, France). All other salts and chemicals were obtained from Sigma-Aldrich or VWR International Ltd.

Results

Benzamil modulation of dendritic Ca^{2+} transients and the I_{AHP} in hippocampal pyramidal neurons

In order to investigate the role of the Na^+/Ca^{2+} exchanger in the feedback regulation of dendritic Ca^{2+} transients by SK channels, whole-cell patch clamp recordings and two-photon Ca^{2+} imaging were performed simultaneously on morphologically identified hippocampal pyramidal neurons in culture, as described previously (Tonini et al., 2013). Back-propagating action potentials (Fig. 1A) were elicited by four somatic current injections of 10-ms-long depolarizing pulses at 20 Hz in neurons that were internally perfused via a patch pipette containing the high affinity Ca^{2+} indicator Fluo-4. The time course of the increase in fluorescence in the proximal region of the apical dendrite reflects the increase in the intracellular free Ca^{2+} concentration (Fig. 1A, control). Under control conditions, the fluorescence transients decay with a time constant of 362 ± 53 ms (Fig. 1B, C, control), comparable to our earlier report (Tonini et al., 2013).

Ca^{2+} transients triggered by backpropagating action potentials in the proximal dendrites of hippocampal neurons are increased and prolonged following inhibition of the I_{AHP} current (Tonini et al., 2013). The time course of decay of Ca^{2+} transients in dendrites depends on the rate of Ca^{2+} clearance (Scheuss et al., 2006). Na^+/Ca^{2+} exchangers, which are responsible in part for the Ca^{2+} clearance from the cytosol, are expressed in the dendrites of primary hippocampal neurons (Kiedrowski, 2004; Kip et al., 2006). The increased duration of Ca^{2+} signals observed upon I_{AHP} suppression as a consequence of SK channel inhibition (Tonini et al., 2013) might be due to a reduced activity of the Na^+/Ca^{2+} exchangers, which are inhibited by elevated Ca^{2+} levels (Scheuss et al., 2006). If this were the case, inhibition of the Na^+/Ca^{2+} exchanger by benzamil would be expected to mimic and occlude the SK channel mediated increase of the duration of the Ca^{2+} transients.

Consistent with this hypothesis, we found that 30 µM benzamil slowed the decay of the fluorescence transients in the proximal region of the apical dendrite by 60 ± 19% (Fig. 1A-C; control: τ = 362 ± 53 ms, benzamil: τ = 603 ± 135 ms, n = 6, P = 0.044;) and increased the amount of Ca^{2+} entering the cell (Fig. 1B), as estimated by the area under the curve of the fluorescent transient, by 44 ± 8 % (Fig. 1D; n = 6, P = 0.006). The increase in duration of Ca^{2+} transients is expected upon inhibition of the Na^+/Ca^{2+} exchanger by benzamil. Moreover, the amplitude of the fluorescent transients increased to 118 ± 6% (Fig. 1B and E; n = 6, P = 0.017), which also contributed to the overall increase in intracellular Ca^{2+} concentration in the proximal dendrites.

The afterpotentials following each action potential in the 20 Hz train were shifted by benzamil in the depolarizing direction (Fig. 1A). These effects of benzamil on the amplitude of Ca^{2+} transients and afterpotentials closely resembled those seen in the presence of the SK channel inhibitors apamin and d-tubocurarine (dTC) (Tonini et al., 2013). This raised the question as to whether benzamil, beside inhibiting the Na^+/Ca^{2+} exchanger, also inhibited neuronal SK channels.

To test this hypothesis, we investigated its effect on the SK-mediated afterhyperpolarizing current I_{AHP} in hippocampal neurons (Stocker et al., 1999). I_{AHP} was recorded as a tail current at -50 mV following a somatic depolarizing voltage step to + 30 mV to elicit Ca^{2+} influx through voltage-gated Ca^{2+} channels. I_{AHP} was present in all cells tested and had a mean amplitude of 94 ± 10 pA (Fig. 2A and C, n = 11) and a time constant of decay of 369 ± 49 ms (Fig. 2A, n = 11). Within 6 minutes, benzamil (30 µM) completely suppressed both I_{AHP} peak amplitude (104 ± 3%, n=11) and area under the curve (100 ± 7 %, n=11), corresponding to amount of charge transported (Fig. 2A-C). Wash out was incomplete, with a maximum of 31 % (15 ± 6%, n=4) of the amplitude and 35 % (20 ± 12%, n=4) of the area under the curve recovered (Fig. 2A-C). Application of the SK channel inhibitor dTC (100 µM) in the presence of benzamil did not produce any further decrease of I_{AHP}, indicating that SK channels were already fully inhibited (Fig. 2B, C). The inhibition of the neuronal SK-mediated I_{AHP}, however, was accompanied by a clear reduction in the peak of the Ca^{2+} currents preceding the I_{AHP} (Fig. 2A, insets), suggesting that benzamil inhibited the voltage-gated Ca^{2+} currents. This was further supported by inhibition of the total voltage-gated calcium currents in CA1 pyramidal neurons from P6-P7 slices (27.9 ± 3.5%; n=8; Fig. 2D-E) by benzamil (30 µM). This inhibition, as well as the inhibition of the I_{AHP}, was not reversible. Altogether, these results prompted the question as to whether the observed reduction of I_{AHP} was caused by benzamil indirectly, due to a reduction in Ca^{2+} entry through the voltage-gated Ca^{2+}-channels, or directly by inhibiting SK channels.

Benzamil inhibition of heterologously expressed SK channels

In order to elucidate whether benzamil exerts a direct inhibitory action on SK channels, we recorded currents from recombinant SK channels expressed in HEK293 cells. We first tested rat SK2 (rSK2) channels, because I_{AHP} in the hippocampus is most likely mediated by SK channels containing the SK2 subunit (Bond et al., 2004; Stocker et al., 1999). In the whole-cell configuration, SK channels were activated by 1 µM free Ca^{2+} in the patch pipette, and SK currents were recorded using a voltage ramp from -140 to +60 mV in a high extracellular K^+ solution. This permitted analysis of linear inward currents through SK channels because outward currents show rectification (Nolting et al., 2007).

The inward currents at -80 mV had an amplitude of -17.7 ± 0.7 nA (n = 61). At the end of the recordings 0.2 – 1 mM dTC was applied to block the SK channels, ensuring that the observed currents resulted predominantly from the activation of SK channels. A small residual current left after dTC application (-0.8 ± 0.06 nA) was a non-SK channel dependent leak current. The reversal potential of the SK mediated current was continuously monitored and was found to be, as predicted for a potassium conductance, 3.1 ± 0.3 mV (n = 61).

The application of 30 μM benzamil, at the same concentration used on hippocampal neurons, suppressed rSK2 currents by 26 ± 1.2 % (n = 10; Fig. 3A, B and E). This suggests that the complete inhibition of the SK-mediated I_{AHP} by benzamil observed in neurons was probably due to the combined inhibition of SK channels and voltage-gated Ca^{2+} channels. Further analysis of the inhibition by benzamil showed a decrease in rSK2 currents in a concentration dependent manner, with 70 μM benzamil (Fig. 3C-E) inhibiting the inward current at -80 mV by ~50% (IC_{50} = 67 μM; 95% CI, 63-73 μM). The Hill coefficient was -1.4 (Fig. 1E), indicating little or no co-operativity for the inhibitory action of benzamil on rSK2 channels. Full inhibition of rSK2 currents was achieved with 1 mM benzamil. Maximal inhibition of the current by benzamil and almost full recovery (89 ± 1.4 %, n = 49) were achieved within minutes (Fig. 3B and D) suggesting a diffusion-controlled mechanism for the rSK2 inhibition.

The unexpected inhibitory action of benzamil on rSK2 channels, and the fact that other SK channel inhibitors, such as apamin, tamapin and dTC, show different potencies on distinct SK channel subtypes (Pedarzani and Stocker, 2008), suggest that benzamil might inhibit SK channels formed by other homologous subunits to a different extent. The effects of benzamil on homomeric human SK1 (hSK1) and rat SK3 (rSK3) channels stably expressed in HEK293 cell lines were therefore investigated. 30 μM benzamil produced a nearly half-maximal inhibition of hSK1 (IC_{50} = 35 μM, Fig. 4A and C) and rSK3 (IC_{50} = 48 μM, Fig. 4B and C) inward currents at -80 mV, showing a potency comparable to that observed for rSK2.

Benzamil inhibition depends on the extracellular [K^+] and membrane voltage

The recording conditions of the neuronal SK-mediated I_{AHP} and recombinant SK currents differ in terms of the ionic composition of intra- and extracellular solutions and the membrane potential at which the currents were measured (outward current at -50 mV in neurons; inward current at -80 mV in HEK293 cells). In particular, the high concentration of extracellular K^+ used for the recordings of recombinant SK currents differs from the physiological extracellular [K^+] and might affect the inhibitory action of benzamil, preventing a meaningful comparison between the data obtained for native and recombinant SK currents. We therefore examined whether benzamil

inhibition of SK currents was affected by the extracellular K^+ concentration or the membrane potential.

Outward currents mediated by rSK2 channels expressed in HEK293 cells were recorded in physiological extracellular [K^+] (4 mM) at +20 and +40 mV in the absence and presence of benzamil (Fig. 5A). Under these ionic conditions, SK2 currents reversed at -83.3 ± 0.6 mV (n = 9) and were half maximally inhibited by 70 μM benzamil at +20 mV (I/I_{max}= 0.48 ± 0.03, n = 7) and at +40 mV (I/I_{max}= 0.55 ± 0.04, n = 7) (Fig. 5 A, B and E). This degree of inhibition was not significantly different from the inhibition observed in high extracellular [K^+] at either of the voltages (+20 mV: I/I_{max}= 0.47 ± 0.03; +40 mV: I/I_{max}= 0.49 ± 0.02; n = 6; P = 0.9 and 0.2 respectively; Fig. 5 C, D and E) This indicates that benzamil inhibition of outward currents at these potentials is not affected by either the extracellular [K^+] or inward rectification of SK channels. However, in the presence of physiological extracellular [K^+] application of benzamil leads to a less pronounced inward rectification at positive potentials. This is exemplified by the mean current ratio at -40 and +40 mV, corresponding respectively to the linear and rectifying phases of the current-voltage relation (Fig. 5A), that was significantly reduced after application of benzamil ($ratio_{-40/+40}$: control = 0.55 ± 0.04, benzamil = 0.41 ± 0.02, n = 6; P = 0.006). In high extracellular K^+ solution benzamil had a similar, albeit less pronounced effect on current rectification at positive membrane potentials ($ratio_{-40/+40}$: control = 2.01 ± 0.08, benzamil = 1.78 ± 0.09, n = 6; P = 0.03).

After establishing that the extracellular [K^+] does not affect the inhibitory effect of benzamil on SK2 currents at positive membrane potentials, we investigated possible differences at negative membrane potentials, where the current-voltage relation is more linear. SK2 current suppression by 70 μM benzamil was close to half maximal at all voltages measured in high extracellular [K^+] (P = 0.7, one way ANOVA). In the presence of 4 mM extracellular K^+, benzamil had a greater effect at negative compared with positive potentials (P < 0.0001, one way ANOVA), revealing a voltage-dependent action of the drug under physiological ionic conditions (Fig. 5B, D and E). Inward currents at -100, -120 and -140 mV in 4 mM extracellular [K^+] were inhibited to the same extent as outward currents at -60, -40 and -20 mV (P > 0.05 Bonferroni post-test, data not shown), indicating that the strength of inhibition was independent of the direction of ion flow. The fraction of rSK2 current left after benzamil at negative voltages was smaller in physiological extracellular [K^+] than in high extracellular [K^+] (Fig. 5E; ** p < 0.001, two way ANOVA and Bonferroni post-test, n = 6-7).

The smaller current fraction at negative voltages in physiological [K^+] gradient (Fig. 5E) suggests a leftward shift in the concentration-response curve with a moderate decrease in the IC_{50} of benzamil to ~40 μM. This could explain the slightly stronger suppression of neuronal SK

currents observed at a benzamil concentration of 30 μM compared to that observed for recombinant rSK2 channels.

In a separate set of experiments, we tested whether reversing the polarity of the ramp protocol and therefore the direction of K^+ ion flow at the outset of the experiment would affect the strength of inhibition of rSK2 currents by benzamil in high extracellular [K^+]. Current reduction by benzamil was the same for upward and downward ramp protocols (I/I_{max}(-80 mV): upward ramp = 0.49 ± 0.02, n = 6, downward ramp = 0.47 ± 0.02, n = 7; P = 0.6; data not shown), suggesting that the potassium ion flow does not influence the potency of inhibition.

In summary, inhibition of rSK2 currents by benzamil is slightly decreased by high extracellular [K^+] at negative membrane potentials and it increases at more depolarized membrane voltages under physiological [K^+] gradient conditions. These findings do not appear to be linked to drug-induced changes in rectification, which were observed in both physiological and high [K^+]. Similarly, the direction of current flow does not seem to influence the potency of inhibition in symmetric [K^+] conditions.

Amiloride is a lower potency inhibitor of SK channels

Benzamil was originally developed as a potent analogue of the K^+-sparing diuretic amiloride (Cragoe et al., 1967). The addition of the hydrophobic benzyl moiety to the guanidinium group of amiloride greatly enhanced the selectivity and inhibitory potency of the drug on epithelial Na^+ channels and Na^+/Ca^{2+} exchangers compared to the parent compound (Kleyman and Cragoe, 1988). Given the inhibitory action of benzamil on SK channels, we sought to establish whether amiloride could similarly lead to SK channel inhibition, and with what potency. Amiloride (70 μM) produced an inhibition of rSK2 currents by 8.6 ± 0.5 % (n = 5; Fig 6A, B and E). At 500 μM it inhibited the currents by 64.4 ± 1.3 % (n = 8; Fig. 6C, D and E). This suggests an IC_{50} of ~300 μM of amiloride for the inhibition of rSK2 currents and that benzamil is 4.5 times more potent (Fig. 6E). The inhibition of rSK2 currents by amiloride has a similar time-course to benzamil and was readily and fully reversible (99 ± 0.7 %, n = 11; Fig. 6B and D).

Discussion

Benzamil affects multiple ionic mechanisms involved in the regulation of dendritic Ca^{2+} transients in hippocampal neurons

This study shows that benzamil, commonly used as an inhibitor of the Na^+/Ca^{2+} exchanger (Kaczorowski et al., 1988), regulates transient Ca^{2+} elevations in neurons through the inhibition of multiple targets, including SK channels.

We have previously shown that SK channels limit the amplitude and duration of Ca^{2+} transients induced by back-propagating action potentials in the proximal apical dendrites of hippocampal neurons (Tonini et al., 2013). To investigate a potential functional interaction between SK channels and Ca^{2+} extrusion mechanisms in the regulation of the duration of dendritic Ca^{2+} transients, in this study we used benzamil to target the Na^+/Ca^{2+} exchanger, as previously done in hippocampal (Lorincz et al., 2007) and other cortical neurons (Goldberg et al., 2003; Markram et al., 1995). While, as expected, benzamil prolonged the duration of dendritic Ca^{2+} transients as a consequence of inhibition of Ca^{2+} extrusion through the Na^+/Ca^{2+} exchanger, it also unexpectedly enhanced the amplitude of the Ca^{2+} transients. Our findings are in agreement with previous observations obtained in the dendritic shafts of CA1 (Lorincz et al., 2007) and subicular (Srinivas and Sikdar, 2008) pyramidal neurons, where Ca^{2+} transients elicited by repeated synaptic stimulation or back-propagating action potentials presented an increase in both amplitude and duration in response to the application of benzamil. The increase in Ca^{2+} transient amplitude obtained in response to the application of both benzamil (this study) and SK channel inhibitors (Tonini et al., 2013), together with the effect of benzamil on the spike afterpotentials, suggested that part of the effect of benzamil might be due to an action on neuronal SK channels. This hypothesis was corroborated by our finding that benzamil, at the same concentration used in the Ca^{2+} imaging experiments (30 μM), inhibits the SK-mediated I_{AHP} in hippocampal neurons. However, these experiments revealed also a concomitant inhibitory effect of benzamil on the voltage-gated Ca^{2+} currents activated to elicit I_{AHP}, consistent with the reported action of benzamil on voltage-gated Ca^{2+} channels in other systems (Garcia et al., 1990). The concomitant reduction of voltage-gated Ca^{2+} currents might explain why the increase in Ca^{2+} transient amplitude associated with SK channel inhibition by benzamil (this study) was smaller in comparison to previous results with the SK channel inhibitor d-tubocurarine (Tonini et al., 2013). In addition, the voltage-clamp experiments on the I_{AHP} in hippocampal neurons were not performed in the presence of KCNQ channel inhibitors, leaving the possibility that benzamil might affect also the KCNQ-mediated I_M beside I_{AHP}. However, the potential overlapping effect on I_M is minimal in primary hippocampal neurons under the experimental conditions used in this

study, as in previously published similar experiments I_{AHP} was shown to be suppressed by 81±6% and 89±3% by the SK-inhibitors apamin and dTC (Tonini et al., 2013). On one hand the findings presented here reveal that benzamil is of limited use as a pharmacological tool to draw conclusions on the role of Na^+/Ca^{2+} exchangers in regulating Ca^{2+} extrusion from neuronal processes, because it targets other relevant components (SK and voltage-gated Ca^{2+} channels) of the neuronal Ca^{2+} signalling toolkit. On the other hand, they unveil SK channels as a novel potential target for benzamil action.

Benzamil directly inhibits SK channels

The effect of benzamil on the SK-mediated I_{AHP} in hippocampal neurons was suggestive of a direct inhibition of these channels by the compound, but not conclusive due to the concomitant inhibition of voltage-gated Ca^{2+} currents responsible for SK channel activation. Our recordings from recombinant SK channels expressed in HEK cells present definitive evidence of a direct action of benzamil on SK channels. Benzamil inhibited all three types of homomeric SK channels, hSK1, rSK2 and rSK3, with IC_{50} values in the same order of magnitude. To prevent errors in our IC_{50} measurements by time-dependent changes in whole-cell currents, such as the run-up of hSK1 currents (see also Strobaek et al., 2000) and the run-down of rSK3 currents, we allowed currents to stabilize before applying benzamil at different concentrations. Similar to benzamil, many inhibitors of SK channels, such as quaternary salts of bicuculline, fluoxetine, NS8593, TEA, methyl-laudanosine and –noscapine, exhibit similar potency on all three homomeric SK channel subtypes (Pedarzani and Stocker, 2008). Their mechanism of inhibition of SK channels varies: pore interactions and block have been proposed for TEA (Dilly et al., 2013; Ishii et al., 1997; Monaghan et al., 2004), methyl-laudanosine (Badarau et al., 2014) and, at the level of the outer pore vestibule, for quaternary salts of bicuculline (Khawaled et al., 1999), while NS8593 acts intracellularly on the Ca^{2+} gating molecular machinery (Sorensen et al., 2008). SK channel subtype specificity and mechanism of action are different in the case of apamin, which displays highest affinity for SK2 and lowest for SK1 channels (Pedarzani and Stocker, 2008) and a complex, allosteric inhibitory mechanism, as the toxin interacts with amino acids both within (Ishii et al., 1997; Nolting et al., 2007) and outside the pore region (Lamy et al., 2010; Nolting et al., 2007; Weatherall et al., 2011). The molecular determinants of benzamil sensitivity in SK channels are as yet unknown and merit further study. Furthermore, we cannot discard the possibility that the actual strength of benzamil inhibition be different in neurons, where SK subunits may combine to form heteromeric SK channels, compared with the homomeric channels we expressed in HEK293 cells.

We found that the inhibition of SK channels by benzamil is affected by the membrane potential under physiological [K^+] conditions. The effect is reminiscent of the voltage-dependent block described for bicuculline (Khawaled et al., 1999) and dTC (Strobaek et al., 2000), which was however observed in high extracellular [K^+]. These studies hypothesized that when the current flow changed from inward to outward in a voltage range from -60 to +80 mV, the movement of K^+ through the pore destabilized drug binding to an extracellular site in or near the pore, decreasing the fraction of current blocked at positive potentials. The IC_{50} for benzamil also seems to increase with larger outward currents at positive voltages under physiological ionic conditions, and to decrease with negative potentials, but unlike bicuculline and dTC, this is not observed under high extracellular [K^+] conditions, (i.e. the IC_{50} remains the same at every voltage and current direction examined). This suggests that the change in the potency of benzamil is linked to the extracellular [K^+] and cannot be simply explained by the 'knock off' effect of K^+ ions moving outwards through the pore. The current-voltage relationship of SK channels is also modified in the presence of benzamil, as rectification is reduced at half maximal inhibitory concentrations in both physiological and high extracellular [K^+]. Inward rectification of SK channels at positive potentials arises partly from intracellular Ca^{2+} and Mg^{2+} block near the selectivity filter (Soh and Park, 2002) and partly from an intrinsic property linked to electrostatic interactions of charged residues near the inner pore (Li and Aldrich, 2011). Taken together, the voltage-dependence of SK channel inhibition and the changes in rectification observed upon benzamil application suggest that the binding site of benzamil on SK channels might be close to the channel pore, leading to the observed interaction with rectification by divalent cations and the transmembrane movement of K^+ ions. Although benzamil and amiloride are highly lipophilic compounds, able to cross biological membranes (Kleyman and Cragoe, 1988), the inhibitory effect of both drugs on SK channels is fast and mostly reversible, suggesting an extracellular mode of action. This would be in strong agreement with their proposed inhibitory mechanism on epithelial Na^+ channels, where the charged guanidinium group, mostly responsible for channel block (Cuthbert, 1976) binds residues in the external vestibule with a K_i that is sensitive to the extracellular [Na^+] and voltage (Kellenberger et al., 2003; McNicholas and Canessa, 1997). Amino acids in all three subunits of the Na^+ channel are involved in the formation of a binding pocket for amiloride and benzamil (Kellenberger et al., 2003; McNicholas and Canessa, 1997). The different effects of benzamil and amiloride on SK channels suggest that additional hydrophobic interactions of the benzene group of benzamil might underlie its greater potency over amiloride, as it has been proposed for epithelial Na^+ channels (Kellenberger et al., 2003). In the light of this work on the inhibitory action of amiloride and benzamil on epithelial Na^+ channels, the results presented in this study make

therefore further investigations on the precise molecular determinants of benzamil binding and its inhibitory mechanism of action on SK channels of particular interest.

In conclusion, although benzamil has been used extensively as a tool to inhibit Na^+-dependent Ca^{2+} extrusion processes in neurons, our results demonstrate that, in addition to the well-recognized actions of benzamil on the plasma membrane exchanger, it also inhibits SK and Ca^{2+} channels in a similar range of concentrations. Our results prompt to extreme caution when drawing conclusions on the role of Na^+/Ca^{2+} exchanger-mediated Ca^{2+} extrusion in neurons based on the sole use of benzamil.

Acknowledgements

The authors gratefully acknowledge J. Dempster for supplying the Strathclyde Electrophysiology Software.

This work was supported by an EMBO short-term fellowship (EMBO ASTF 137.00-03) and a Human Frontier Science Program (HFSP) short-term fellowship (ST00323/2002-C) to R. Tonini. P. Pedarzani acknowledges support by the HFSP (RGP0013/2010).

References

Badarau, E., Dilly, S., Wouters, J., Seutin, V., Liegeois, J. F., 2014. Chemical modifications of the N-methyl-laudanosine scaffold point to new directions for SK channels exploration. Bioorg. Med. Chem. Lett. 24, 5616-5620. https://doi.org/10.1016/j.bmcl.2014.10.083

Blanton, M. G., Lo Turco, J. J., Kriegstein, A. R., 1989. Whole cell recording from neurons in slices of reptilian and mammalian cerebral cortex. J Neurosci Methods 30, 203-210

Bloodgood, B. L., Sabatini, B. L., 2007. Nonlinear regulation of unitary synaptic signals by $CaV_{2.3}$ voltage-sensitive calcium channels located in dendritic spines. Neuron 53, 249-260. https://doi.org/10.1016/j.neuron.2006.12.017

Bond, C. T., Herson, P. S., Strassmaier, T., Hammond, R., Stackman, R., Maylie, J., Adelman, J. P., 2004. Small conductance Ca^{2+}-activated K^+ channel knock-out mice reveal the identity of calcium-dependent afterhyperpolarization currents. J. Neurosci. 24, 5301-5306. https://doi.org/10.1523/JNEUROSCI.0182-04.2004

Brini, M., Cali, T., Ottolini, D., Carafoli, E., 2014. Neuronal calcium signaling: function and dysfunction. Cell. Mol. Life. Sci. 71, 2787-2814. https://doi.org/10.1007/s00018-013-1550-7

Cai, X., Liang, C. W., Muralidharan, S., Kao, J. P., Tang, C. M., Thompson, S. M., 2004. Unique roles of SK and Kv4.2 potassium channels in dendritic integration. Neuron 44, 351-364. https://doi.org/10.1016/j.neuron.2004.09.026

Cragoe, E. J., Jr., Woltersdorf, O. W., Jr., Bicking, J. B., Kwong, S. F., Jones, J. H., 1967. Pyrazine diuretics. II. N-amidino-3-amino-5-substituted 6-halopyrazinecarboxamides. J. Med. Chem. 10, 66-75

Cueni, L., Canepari, M., Lujan, R., Emmenegger, Y., Watanabe, M., Bond, C. T., Franken, P., Adelman, J. P., Luthi, A., 2008. T-type Ca^{2+} channels, SK2 channels and SERCAs gate sleep-related oscillations in thalamic dendrites. Nat. Neurosci. 11, 683-692. https://doi.org/10.1038/nn.2124

Cuthbert, A. W., 1976. Importance of guanidinium groups of blocking sodium channels in epithelia. Mol. Pharmacol. 12, 945-957

Dai, X. Q., Ramji, A., Liu, Y., Li, Q., Karpinski, E., Chen, X. Z., 2007. Inhibition of TRPP3 channel by amiloride and analogs. Mol. Pharmacol. 72, 1576-1585. https://doi.org/10.1124/mol.107.037150

Dilly, S., Philippart, F., Lamy, C., Poncin, S., Snyders, D., Seutin, V., Liegeois, J. F., 2013. The interactions of apamin and tetraethylammonium are differentially affected by single mutations in the pore mouth of small conductance calcium-activated potassium (SK) channels. Biochem. Pharmacol. 85, 560-569. https://doi.org/10.1016/j.bcp.2012.12.015

Faber, E. S., 2010. Functional interplay between NMDA receptors, SK channels and voltage-gated Ca^{2+} channels regulates synaptic excitability in the medial prefrontal cortex. J. Physiol. (Lond.) 588, 1281-1292. https://doi.org/10.1113/jphysiol.2009.185645

Fung, M. L., Haddad, G. G., 1997. Anoxia-induced depolarization in CA1 hippocampal neurons: role of Na^+-dependent mechanisms. Brain Res. 762, 97-102

Garcia, M. L., King, V. F., Shevell, J. L., Slaughter, R. S., Suarez-Kurtz, G., Winquist, R. J., Kaczorowski, G. J., 1990. Amiloride analogs inhibit L-type calcium channels and display calcium entry blocker activity. J. Biol. Chem. 265, 3763-3771

Goldberg, J. H., Tamas, G., Aronov, D., Yuste, R., 2003. Calcium microdomains in aspiny dendrites. Neuron 40, 807-821

Higley, M. J., Sabatini, B. L., 2010. Competitive regulation of synaptic Ca^{2+} influx by D2 dopamine and A2A adenosine receptors. Nat. Neurosci. 13, 958-966. https://doi.org/10.1038/nn.2592

Ishii, T. M., Maylie, J., Adelman, J. P., 1997. Determinants of apamin and *d*-tubocurarine block in SK potassium channels. J. Biol. Chem. 272, 23195-23200

Jones, S. L., Stuart, G. J., 2013. Different calcium sources control somatic versus dendritic SK channel activation during action potentials. J. Neurosci. 33, 19396-19405. https://doi.org/10.1523/JNEUROSCI.2073-13.2013

Jones, S. L., To, M. S., Stuart, G. J., 2017. Dendritic small conductance calcium-activated potassium channels activated by action potentials suppress EPSPs and gate spike-timing dependent synaptic plasticity. eLife 6, e30333. https://doi.org/10.7554/eLife.30333

Jurkowitz, M. S., Altschuld, R. A., Brierley, G. P., Cragoe, E. J., Jr., 1983. Inhibition of Na^{+}-dependent Ca^{2+} efflux from heart mitochondria by amiloride analogues. FEBS Lett. 162, 262-265

Kaczorowski, G. J., Barros, F., Dethmers, J. K., Trumble, M. J., Cragoe, E. J., Jr., 1985. Inhibition of Na^{+}/Ca^{2+} exchange in pituitary plasma membrane vesicles by analogues of amiloride. Biochemistry 24, 1394-1403

Kaczorowski, G. J., Slaughter, R. S., Garcia, M. L., King, V. F., 1988. The role of sodium-calcium exchange in excitable cells. Biochem. Soc. Trans. 16, 529-532

Kapus, A., Lukacs, G. L., Cragoe, E. J., Jr., Ligeti, E., Fonyo, A., 1988. Characterization of the mitochondrial Na^{+}-H^{+} exchange. The effect of amiloride analogues. Biochim. Biophys. Acta 944, 383-390

Kellenberger, S., Gautschi, I., Schild, L., 2003. Mutations in the epithelial Na^{+} channel ENaC outer pore disrupt amiloride block by increasing its dissociation rate. Mol. Pharmacol. 64, 848-856. https://doi.org/10.1124/mol.64.4.848

Khawaled, R., Bruening-Wright, A., Adelman, J. P., Maylie, J., 1999. Bicuculline block of small-conductance calcium-activated potassium channels. Pflugers Arch - Eur. J. Physiol. 438, 314-321. https://doi.org/10.1007/s004240050915

Kiedrowski, L., 2004. High activity of K^{+}-dependent plasmalemmal Na^{+}/Ca^{2+} exchangers in hippocampal CA1 neurons. Neuroreport 15, 2113-2116

Kip, S. N., Gray, N. W., Burette, A., Canbay, A., Weinberg, R. J., Strehler, E. E., 2006. Changes in the expression of plasma membrane calcium extrusion systems during the maturation of hippocampal neurons. Hippocampus 16, 20-34. https://doi.org/10.1002/hipo.20129

Kleyman, T. R., Cragoe, E. J., Jr., 1988. Amiloride and its analogs as tools in the study of ion transport. J. Membr. Biol. 105, 1-21

Lamy, C., Goodchild, S. J., Weatherall, K. L., Jane, D. E., Liegeois, J. F., Seutin, V., Marrion, N. V., 2010. Allosteric block of $K_{Ca}2$ channels by apamin. J. Biol. Chem. 285, 27067-27077. https://doi.org/10.1074/jbc.M110.110072

Lane, J. W., McBride, D. W., Jr., Hamill, O. P., 1992. Structure-activity relations of amiloride and its analogues in blocking the mechanosensitive channel in Xenopus oocytes. Br. J. Pharmacol. 106, 283-286

Li, W., Aldrich, R. W., 2011. Electrostatic influences of charged inner pore residues on the conductance and gating of small conductance Ca^{2+} activated K^+ channels. Proc. Natl. Acad. Sci. U. S. A. 108, 5946-5953. https://doi.org/10.1073/pnas.1103090108

Lobner, D., Lipton, P., 1993. Intracellular calcium levels and calcium fluxes in the CA1 region of the rat hippocampal slice during in vitro ischemia: relationship to electrophysiological cell damage. J. Neurosci. 13, 4861-4871

Lorincz, A., Rozsa, B., Katona, G., Vizi, E. S., Tamas, G., 2007. Differential distribution of NCX1 contributes to spine-dendrite compartmentalization in CA1 pyramidal cells. Proc. Natl. Acad. Sci. U. S. A. 104, 1033-1038. https://doi.org/10.1073/pnas.0605412104

Markram, H., Helm, P. J., Sakmann, B., 1995. Dendritic calcium transients evoked by single back-propagating action potentials in rat neocortical pyramidal neurons. J. Physiol. (Lond.) 485 (Pt 1), 1-20

McNicholas, C. M., Canessa, C. M., 1997. Diversity of channels generated by different combinations of epithelial sodium channel subunits. J. Gen. Physiol. 109, 681-692

Monaghan, A. S., Benton, D. C., Bahia, P. K., Hosseini, R., Shah, Y. A., Haylett, D. G., Moss, G. W., 2004. The SK3 subunit of small conductance Ca^{2+}-activated K^+ channels interacts with both SK1 and SK2 subunits in a heterologous expression system. J. Biol. Chem. 279, 1003-1009. https://doi.org/10.1074/jbc.M308070200

Ngo-Anh, T. J., Bloodgood, B. L., Lin, M., Sabatini, B. L., Maylie, J., Adelman, J. P., 2005. SK channels and NMDA receptors form a Ca^{2+}-mediated feedback loop in dendritic spines. Nat. Neurosci. 8, 642-649. https://doi.org/10.1038/nn1449

Nolting, A., Ferraro, T., D'Hoedt, D., Stocker, M., 2007. An amino acid outside the pore region influences apamin sensitivity in small conductance Ca^{2+}-activated K^+ channels. J. Biol. Chem. 282, 3478-3486. https://doi.org/10.1074/jbc.M607213200

Page, A. J., Brierley, S. M., Martin, C. M., Hughes, P. A., Blackshaw, L. A., 2007. Acid sensing ion channels 2 and 3 are required for inhibition of visceral nociceptors by benzamil. Pain 133, 150-160. https://doi.org/10.1016/j.pain.2007.03.019

Pedarzani, P., D'Hoedt, D., Doorty, K. B., Wadsworth, J. D., Joseph, J. S., Jeyaseelan, K., Kini, R. M., Gadre, S. V., Sapatnekar, S. M., Stocker, M., Strong, P. N., 2002. Tamapin, a venom peptide from the Indian red scorpion (Mesobuthus tamulus) that targets small conductance Ca^{2+}-activated K^+ channels and afterhyperpolarization currents in central neurons. J. Biol. Chem. 277, 46101-46109. https://doi.org/10.1074/jbc.M206465200

Pedarzani, P., Stocker, M., 2008. Molecular and cellular basis of small- and intermediate-conductance, calcium-activated potassium channel function in the brain. Cell. Mol. Life. Sci. 65, 3196-3217. https://doi.org/10.1007/s00018-008-8216-x

Rudolph, S., Thanawala, M. S., 2015. Location matters: somatic and dendritic SK channels answer to distinct calcium signals. J. Neurophysiol. 114, 1-5. https://doi.org/10.1152/jn.00181.2014

Rusch, A., Kros, C. J., Richardson, G. P., 1994. Block by amiloride and its derivatives of mechano-electrical transduction in outer hair cells of mouse cochlear cultures. J. Physiol. (Lond.) 474, 75-86

Santos-Torres, J., Slimak, M. A., Auer, S., Ibanez-Tallon, I., 2011. Cross-reactivity of acid-sensing ion channel and Na^+-H^+ exchanger antagonists with nicotinic acetylcholine receptors. J. Physiol. (Lond.) 589, 5109-5123. https://doi.org/10.1113/jphysiol.2011.213272

Schellenberg, G. D., Anderson, L., Cragoe, E. J., Jr., Swanson, P. D., 1985. Inhibition of synaptosomal membrane Na^+-Ca^{2+} exchange transport by amiloride and amiloride analogues. Mol. Pharmacol. 27, 537-543

Scheuss, V., Yasuda, R., Sobczyk, A., Svoboda, K., 2006. Nonlinear [Ca^{2+}] signaling in dendrites and spines caused by activity-dependent depression of Ca^{2+} extrusion. J. Neurosci. 26, 8183-8194. https://doi.org/10.1523/JNEUROSCI.1962-06.2006

Siegl, P. K., Cragoe, E. J., Jr., Trumble, M. J., Kaczorowski, G. J., 1984. Inhibition of Na^+/Ca^{2+} exchange in membrane vesicle and papillary muscle preparations from guinea pig heart by analogs of amiloride. Proc. Natl. Acad. Sci. U. S. A. 81, 3238-3242

Soh, H., Park, C. S., 2002. Localization of divalent cation-binding site in the pore of a small conductance Ca^{2+}-activated K^+ channel and its role in determining current-voltage relationship. Biophys. J. 83, 2528-2538. https://doi.org/10.1016/S0006-3495(02)75264-8

Sorensen, U. S., Strobaek, D., Christophersen, P., Hougaard, C., Jensen, M. L., Nielsen, E. O., Peters, D., Teuber, L., 2008. Synthesis and structure-activity relationship studies of 2-(N-substituted)-aminobenzimidazoles as potent negative gating modulators of small conductance Ca^{2+}-activated K^+ channels. J. Med. Chem. 51, 7625-7634. https://doi.org/10.1021/jm800809f

Srinivas, K. V., Sikdar, S. K., 2008. Epileptiform activity induces distance-dependent alterations of the Ca^{2+} extrusion mechanism in the apical dendrites of subicular pyramidal neurons. Eur. J. Neurosci. 28, 2195-2212. https://doi.org/10.1111/j.1460-9568.2008.06519.x

Stocker, M., Krause, M., Pedarzani, P., 1999. An apamin-sensitive Ca^{2+}-activated K^+ current in hippocampal pyramidal neurons. Proc. Natl. Acad. Sci. U. S. A. 96, 4662-4667

Strobaek, D., Jorgensen, T. D., Christophersen, P., Ahring, P. K., Olesen, S. P., 2000. Pharmacological characterization of small-conductance Ca^{2+}-activated K^+ channels stably expressed in HEK 293 cells. Br. J. Pharmacol. 129, 991-999. https://doi.org/10.1038/sj.bjp.0703120

Tonini, R., Ferraro, T., Sampedro-Castaneda, M., Cavaccini, A., Stocker, M., Richards, C. D., Pedarzani, P., 2013. Small-conductance Ca^{2+}-activated K^+ channels modulate action potential-induced Ca^{2+} transients in hippocampal neurons. J. Neurophysiol. 109, 1514-1524. https://doi.org/10.1152/jn.00346.2012

Trusel, M., Cavaccini, A., Gritti, M., Greco, B., Saintot, P. P., Nazzaro, C., Cerovic, M., Morella, I., Brambilla, R., Tonini, R., 2015. Coordinated Regulation of Synaptic Plasticity at Striatopallidal and Striatonigral Neurons Orchestrates Motor Control. Cell Rep. 13, 1353-1365. https://doi.org/10.1016/j.celrep.2015.10.009

Uchikado, H., Tanaka, E., Yamamoto, S., Isagai, T., Shigemori, M., Higashi, H., 2000. Na^+/Ca^{2+} exchanger activity induces a slow DC potential after in vitro ischemia in rat hippocampal CA1 region. Neurosci. Res. 36, 129-140

Weatherall, K. L., Seutin, V., Liegeois, J. F., Marrion, N. V., 2011. Crucial role of a shared extracellular loop in apamin sensitivity and maintenance of pore shape of small-conductance calcium-activated potassium (SK) channels. Proc. Natl. Acad. Sci. U. S. A. 108, 18494-18499. https://doi.org/10.1073/pnas.1110724108

Yu, F. H., Shull, G. E., Orlowski, J., 1993. Functional properties of the rat Na/H exchanger NHE-2 isoform expressed in Na/H exchanger-deficient Chinese hamster ovary cells. J. Biol. Chem. 268, 25536-25541

Figures and Legends

Figure 1

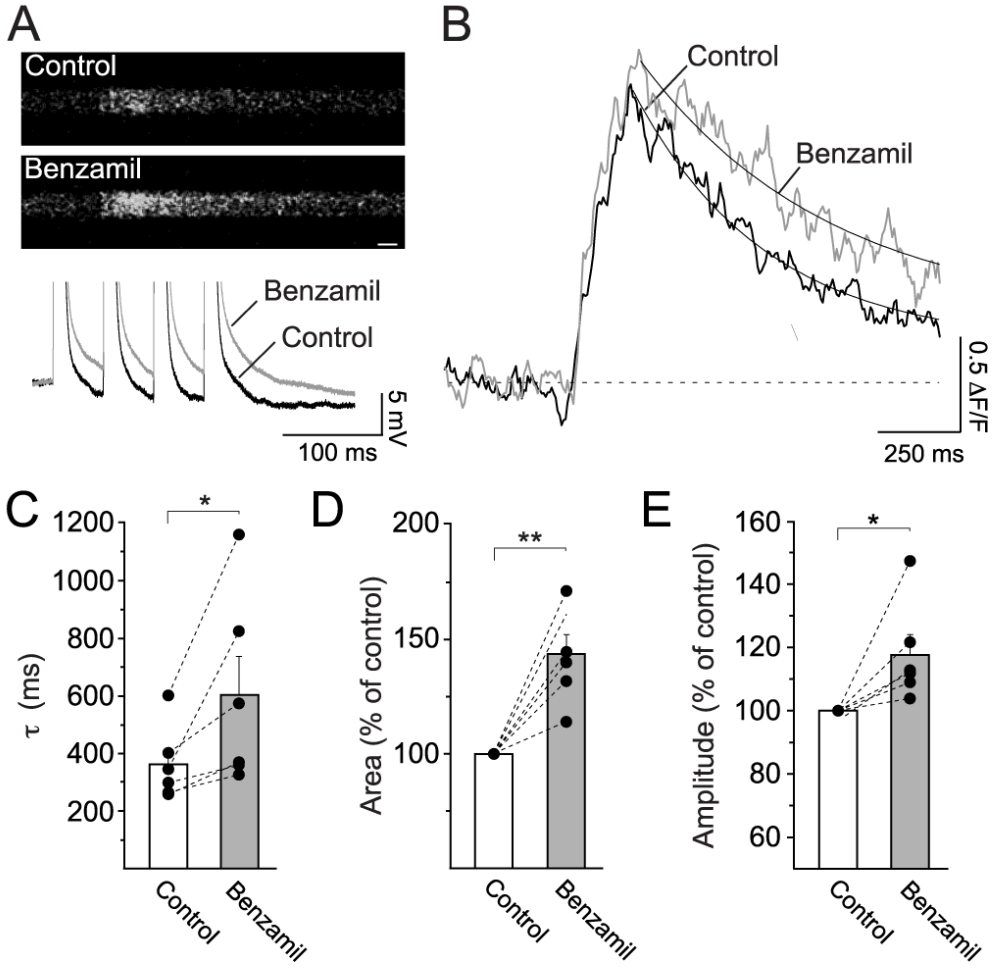

Figure 1. Effects of benzamil on dendritic Ca^{2+} transients in cultured hippocampal neurons.

A) Representative two-photon line scan images of the proximal region of a dendritic process of a pyramidal neuron. Fluo 4 fluorescence (20 μM) was measured in response to a train of 4 back-propagating action potentials at 20 Hz (lower panel, truncated) under control conditions (upper panel) and upon application of benzamil (30 μM; middle panel, scale bar: 100 ms). **B**) Relative change in basal fluorescence due to Ca^{2+} influx in the dendritic process in **A** measured in control conditions (black) and in response to bath application of 30 μM benzamil (grey); superimposed lines indicate mono-exponential fits to the decay of the Ca^{2+} transients (control: 402 ms, benzamil: 574 ms). Experiments were performed in the presence of synaptic blockers (DL-AP5 25 μM; NBQX 5 μM). **C**-**E**) Bar diagrams summarizing the increase in time constant of decay (**C**, P = 0.044), area (**D**, P = 0.006) and peak amplitude (**E**, P = 0.017) of the Ca^{2+} transients measured in 6 proximal dendritic processes following application of 30 μM benzamil.

Figure 2

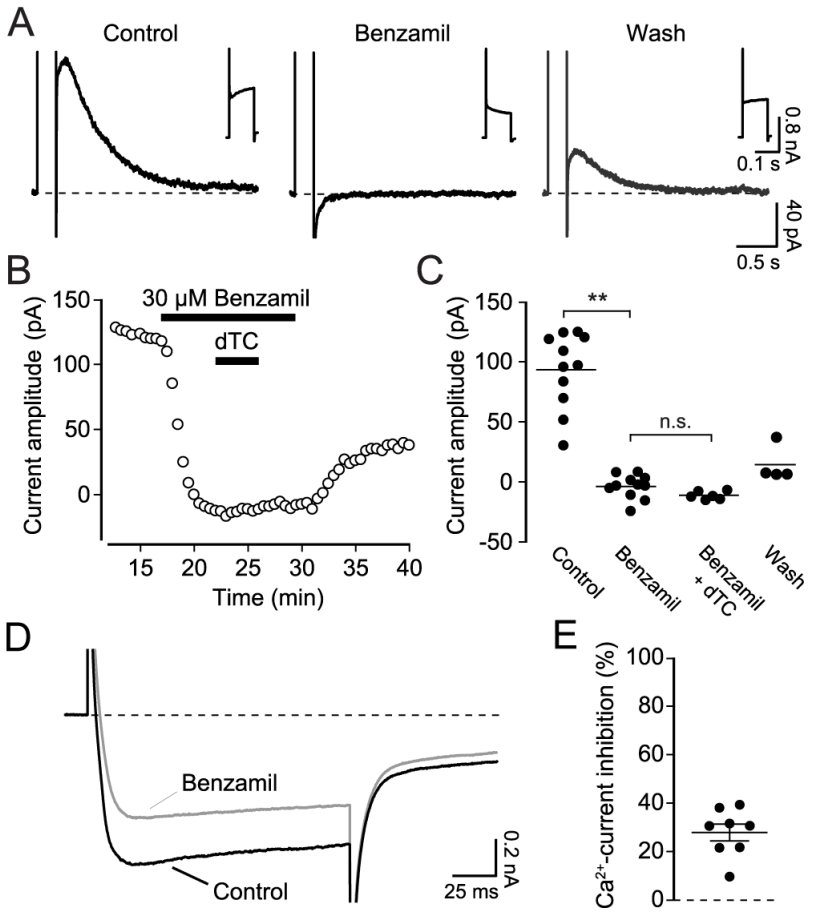

Figure 2. **Suppression of the hippocampal I_{AHP} by benzamil.**

A) Representative whole-cell recordings of the Ca^{2+}-activated K^+ current I_{AHP} generated by the opening of SK channels in response to 200 ms-long depolarizing pulses to +30 mV inducing Ca^{2+} influx through voltage-gated calcium channels in cultured hippocampal neurons. Application of 30 µM benzamil resulted in a partially reversible suppression of I_{AHP} with concomitant changes in the unclamped Ca^{2+} current waveform (insets). Recordings were performed in the presence of synaptic blockers (DL-AP5 25 µM; NBQX 5 µM), TTX 0.5 µM, TEA 1 mM and 8CPT cAMP 50 µM. **B**) Time course of benzamil (30 µM) and d-tubocurarine (dTC; 100 µM) inhibition and wash out of I_{AHP}. **C**) Summary diagram of mean current amplitude in each condition: control, benzamil (30 µM), co-application of benzamil (30 µM) and dTC (100 µM) and washout (wash). Symbols represent individual experiments, n.s. denotes non significant and ** $p < 0.01$. **D**) Representative whole-cell recordings of voltage-gated calcium currents elicited in P6 CA1 pyramidal neurons in response to 150 ms-long depolarizing pulses to +5 mV, before (black trace) and after (grey trace) application of benzamil (30 µM). Recording conditions are specified in Methods. **E**) Summary diagram showing the relative (%) inhibition by benzamil (30 µM) of Ca^{2+} currents recorded from 8 cells (27.9 ± 3.5%; $p < 0.0001$). Symbols represent individual experiments, bars are mean ± SEM.

Figure 3

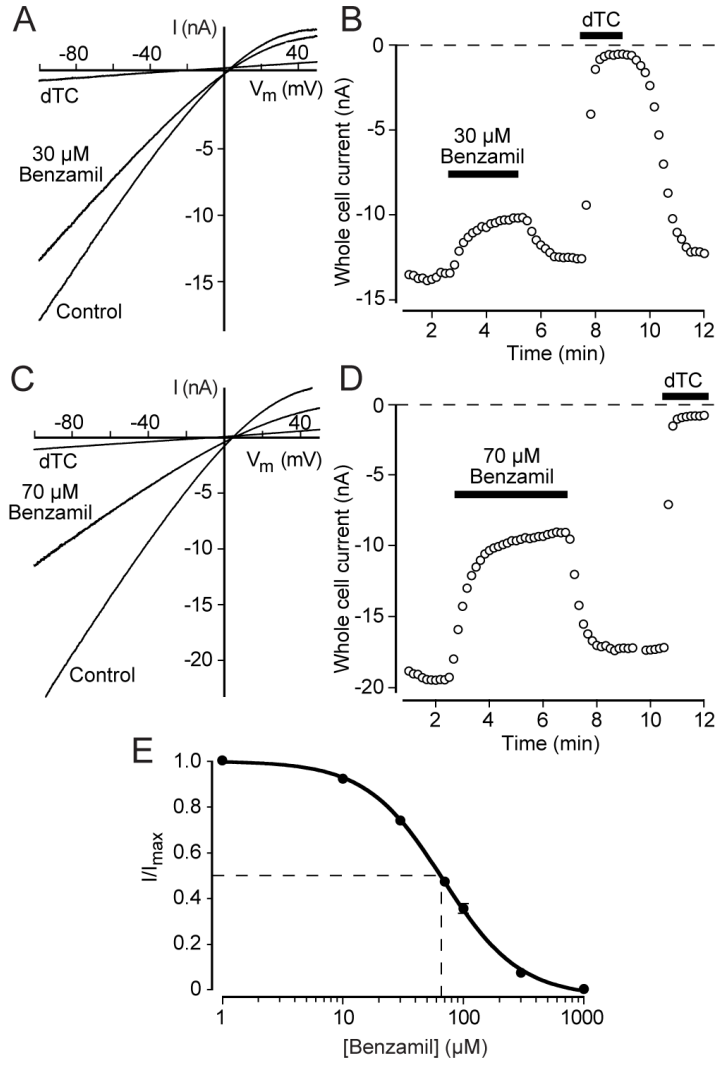

Figure 3. Direct inhibition of homomeric rSK2 channels by benzamil.

A and **C**) Representative recordings of rSK2 currents activated by 1 µM free Ca^{2+} applied through the patch pipette during voltage ramps from -140 to +60 mV from a holding potential of +10 mV show a reduction in both inward and outward K^+ current in the presence of 30 µM (**A**) and 70 µM benzamil (**C**). Application of 200 µM dTC (**A**) and 500 µM dTC (**C**) leaves very small non-SK mediated residual currents. **B** and **D**) Time courses of whole-cell currents corresponding to experiments in **A** and **C** illustrate the benzamil inhibition of inward currents measured at -80 mV, the washout of benzamil at both concentrations and subsequent complete suppression of recovered currents by dTC. **E**) Concentration-response curve for the inhibition of rSK2 channels by benzamil. Data points (n = 6-10) were fitted using a Hill-Langmuir equation and yielded an IC_{50} value of 67 µM (95 % CI: 63-73 µM) and a Hill coefficient of -1.4 (95 % CI: -1.5 to -1.2).

Figure 4

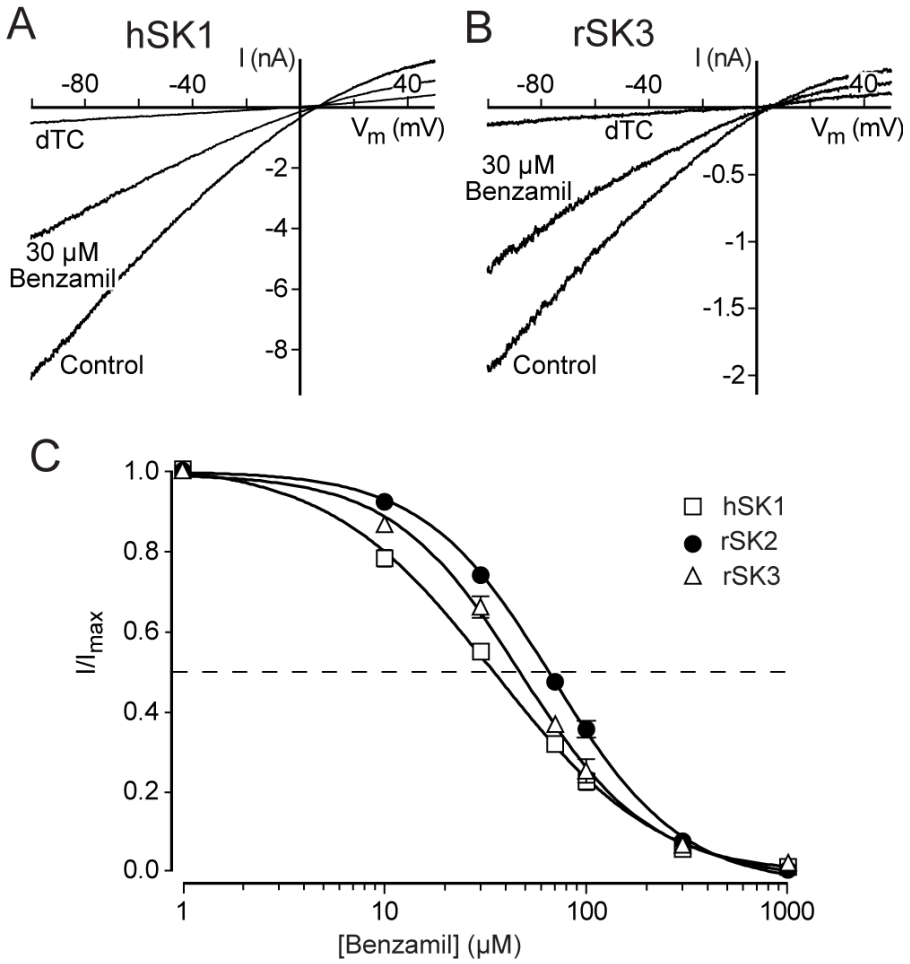

Figure 4. Benzamil inhibits hSK1 and rSK3 channels.

A and **B**) Example current traces illustrate the effect of benzamil (30 µM) on steady state inward and outward currents through hSK1 (**A**) and rSK3 (**B**) homomeric channels. Only small residual currents are left after application of dTC (0.5-1 mM). **C**) Superimposed concentration-response curves for the inhibition of hSK1 (open squares; IC_{50}= 35 µM, 95% CI: 31-39 µM; Hill slope= -1.0, 95% CI: -1.2 to -0.9, n = 5-7), rSK2 (open circles; for data see Fig. 3**E**) and rSK3 (open diamonds; IC_{50}= 48 µM, 95% CI: 42-54 µM; Hill slope= -1.4, 95% CI: -1.6 to -1.1, n = 5-7).

Figure 5

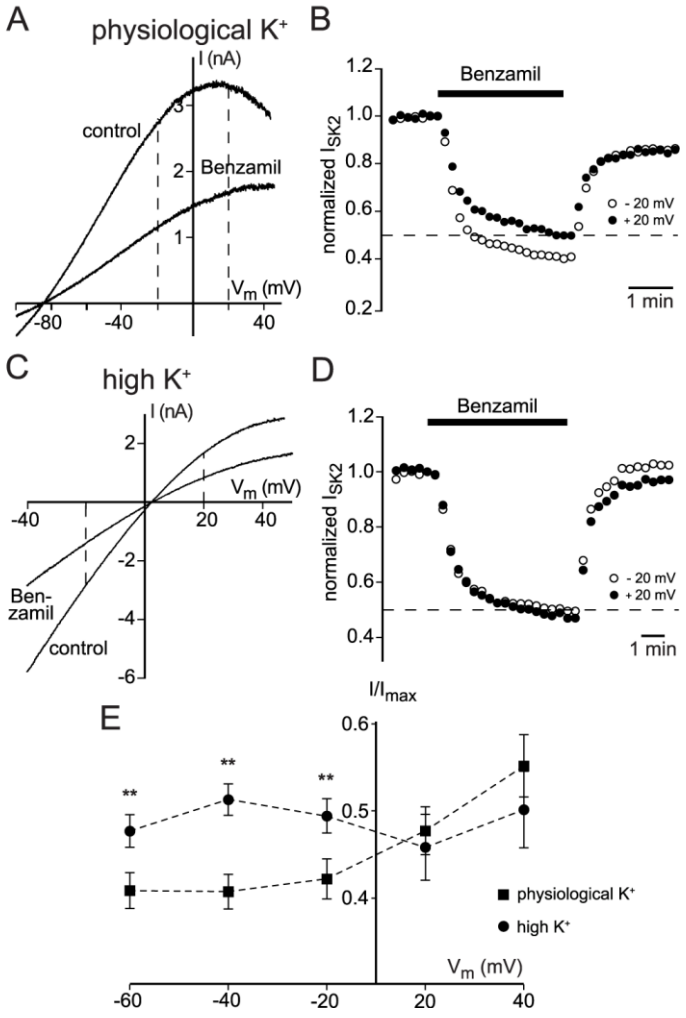

Figure 5. Comparison of rSK2 channel inhibition by benzamil in physiological and high extracellular [K^+].

A and **C**) Representative rSK2 current responses to voltage ramps applied when the extracellular [K^+] was 4 mM (**A**) or 144 mM (**C**) in the presence of benzamil (70 μM). Outward currents are suppressed by benzamil and exhibit less inward rectification at positive potentials in the presence of the drug, particularly in physiological extracellular [K^+] (**A**). Non-SK dependent, dTC-insensitive currents have been subtracted from the traces. **B** and **D**) Normalized time courses of the rSK2 currents recorded in **A** and **C** in the presence of 4 mM (**B**) or 144 mM (**D**) extracellular [K^+]. The time courses show similar effects of benzamil in both ionic conditions at +20 mV (filled circles) and a small but significant increase in the potency of the drug in physiological (4 mM) extracellular [K^+] at -20 mV (open circles). **E**) Fraction of residual rSK2 currents upon benzamil application measured at the indicated voltages shows a greater inhibition by benzamil at negative voltages in physiological extracellular [K^+] (squares) when compared to high extracellular [K^+] (circles) (** $p < 0.001$, two way ANOVA and Bonferroni post-test, n = 6-7).

Figure 6

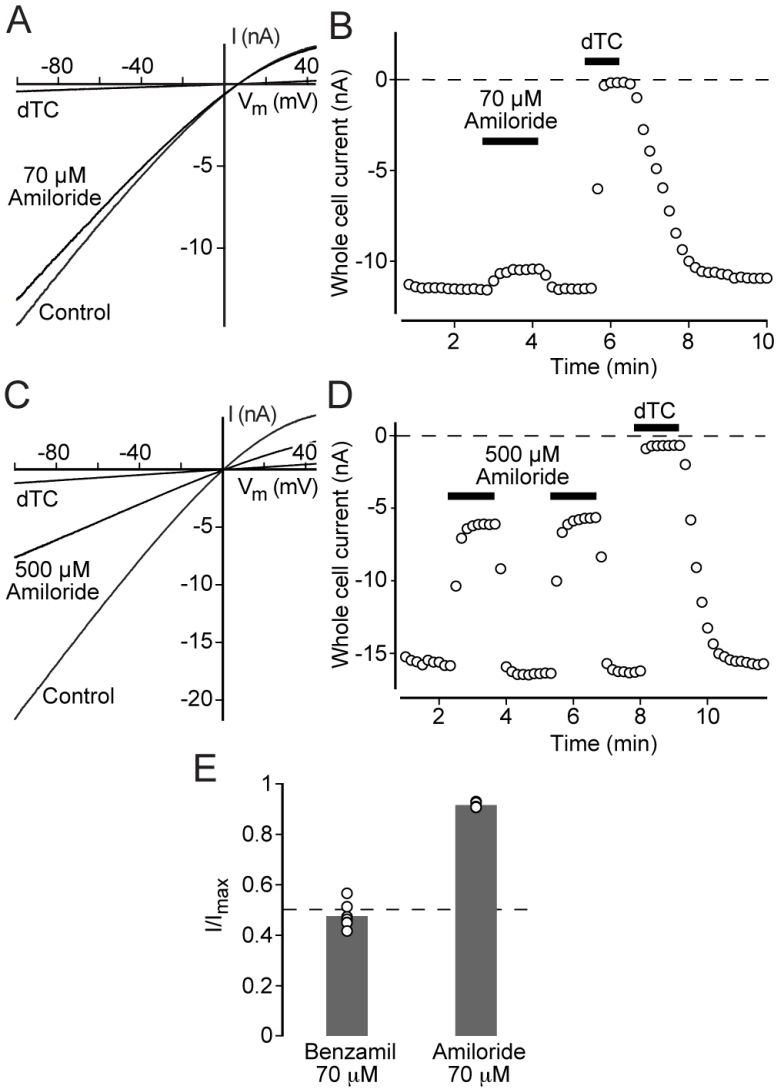

Figure 6. Amiloride suppresses rSK2 currents.

A and **C**) rSK2 current traces show a concentration dependent inhibition of both inward and outward components upon bath application of amiloride 70 µM (**A**; 8.6 ± 0.5% inhibition, n = 5) and 500 µM (**C**; 64.4 ± 1.3% inhibition, n = 8). Residual currents upon rSK2 suppression by dTC (500 µM) were negligible. **B** and **D**) Time courses corresponding to the experiments in **A** and **C** show that amiloride is a fast and reversible inhibitor of rSK2 currents. **E**) Comparison of the overall residual rSK2 currents in the presence of equal concentrations of benzamil and amiloride indicates a several fold lower potency of amiloride compared to benzamil. Symbols represent individual data points ($P < 0.0001$; n = 7 for benzamil and n = 5 for amiloride).